Korean J. Chem. Eng., **27**(1), 299-309 (2010)
DOI: 10.2478/s11814-010-0098-6

Sorption of C. I. Disperse Red 60 in polystyrene and PMMA films and polyester and Nylon 6 textiles in the presence of supercritical carbon dioxide

Sang-Cheol Park*, Dirk Tuma, Sunwook Kim***, Yong Rok Lee*, and Jae-Jin Shim*,†**

*School of Chemical Engineering and Technology, Yeungnam University,
214-1 Dae-dong, Gyeongsan, Gyeongbuk 712-749, Korea
**BAM Federal Institute of Materials Research and Testing, Richard-Willstätter-Str. 11, D-12489 Berlin, Germany
***Department of Chemical Engineering and Bioengineering, University of Ulsan,
Mugeo-2-dong, Nam-gu, Ulsan 680-749, Korea
(*Received 16 September 2009 • accepted 23 November 2009*)

Abstract−C. I. Disperse Red 60 (DR60) was absorbed into polymer films and textile fibers in the presence of supercritical carbon dioxide at pressures between 5 and 33 MPa and at temperatures between 308.2 and 423.2 K. Polystyrene (PS) and poly(methyl methacrylate) (PMMA) films and polyester (polyethylene terephthalate: PET) and Nylon 6 textiles were used as absorbents. The amount of equilibrium sorption of dye increased both with pressure and temperature. The sorption behavior was successfully analyzed with the quasi dual-mode sorption model.

Key words: Supercritical Fluid Dyeing, Supercritical Carbon Dioxide, C. I. Disperse Red 60, Poly(methyl methacrylate), Polystyrene, Polyester, Nylon, Sorption

INTRODUCTION

Since the mid-1980s, applications of supercritical fluids have received significant attention in polymer processing [1] and polymer synthesis [2,3]. Supercritical fluid polymer impregnation [4,5] is one of the prospective applications of polymer processing. As an application of polymer impregnation in supercritical fluids, supercritical fluid dyeing has been investigated since the early 1990s [6-13]. It is an environmentally safe technique, as it may replace the conventional wet-dyeing method. In the wet-dyeing method, the standard polyester textile requires a large amount of dispersing agents and surfactants to overcome the hydrophobicity of the textile itself and the dyestuff. Thus, the dyeing industry discharges a large amount of persistent and little-biodegradable wastewater. In the supercritical fluid dyeing, however, supercritical CO_2 is not only harmless to the environment, as it is inherently nontoxic, but also does not require any water, dispersing agents or surfactants in the dyeing process. Furthermore, the new dyeing process can provide savings in energy, as it neither uses water nor requires any post-drying stage.

So far, only a limited number of studies have been reported for dyeing of polymeric textiles in supercritical fluids, whereas there are an increasing number of studies on measuring the solubility of dyeing agents in supercritical CO_2 [14-27]. Regarding dye sorption, Saus et al. [6] and Gebert et al. [8] reported dyeing of various textiles in supercritical CO_2 for the first time. Chang et al. [9] also reported dyeing of polyester textile fibers and films with C. I. Disperse Blue 60 in the presence of supercritical CO_2. Bach et al. [10] measured the melting point, fiber shrinkage, and strain of polyolefin fibers after treatment in CO_2 under dyeing conditions. They reported a melting point reduction of 5 to 20 K for polyethylene and polypropylene at various pressures. The degree of shrinkage of the fibers was 11-12% and that of the elongation, 13-15%, respectively. They also studied the effect of dye structure on dyeing of polyolefin fibers [10]. West et al. [28] measured dye partitioning and diffusion coefficient in supercritical fluids using the *in situ* UV-VIS spectroscopy. Fleming et al. [29] measured dye diffusion in PET films in supercritical CO_2 using confocal Raman microscopy. The corresponding diffusion coefficient at 20.0 MPa and 353.2 K was $6.75\pm1.01\times10^{-14}$ m^2/s. Santos et al. [30] showed a better incorporation of anthraquinone dyes than of azo dyes for PET films and fibers that were *N,N*-dimethylacrylamide-modified as well UV-radiated in supercritical CO_2. Unfortunately, except for China and Japan, the number of studies on dye sorption in supercritical fluid conditions is not increasing, probably because the initial investment cost for the supercritical fluid dyeing process is much higher than the conventional one and the safety regulations for high pressures are very strict, making the conventional process still profitable. The global restriction on the energy consuming and environmentally hazardous conventional dyeing process has been postponed indefinitely.

To analyze the supercritical fluid dyeing, knowledge on the phase equilibrium of supercritical fluid and polymer is mandatory. Seckner et al. [31] studied an equilibrium of the ternary polystyrene-toluene-ethane system. Shim and Johnston [4,32,33] measured and analyzed the sorption and distribution of toluene, phenanthrene, and anthracene in silicone rubber in the presence of supercritical CO_2. Chang et al. [34] measured the swelling and sorption behavior of various glassy and rubbery polymers in supercritical CO_2. The amount of dye sorption in polymers in the presence of supercritical CO_2 is closely related to both the solubility of dye in the fluid and the distribution of dye between the fluid and the polymer phases. The mobility of dye molecules between polymer chains is generally enhanced due to swelling of polymers in supercritical fluids [4,34].

In this study, sorption of DR60 disperse dye in various polymeric

†To whom correspondence should be addressed.
E-mail: jjshim@yu.ac.kr

materials, i.e., PS, PMMA, PET, and Nylon 6, has been measured in a high-pressure sorption cell, equipped with a magnetic circulation pump. The experimental data have been correlated by a semi-empirical equation similar to the dual-mode sorption model, which is well known for describing the sorption in glassy polymers. From the results of this study, we may better understand the phase equilibrium behavior of ternary systems and predict the dye sorption at other conditions in order to provide the necessary information in designing and operating supercritical fluid dyeing equipment.

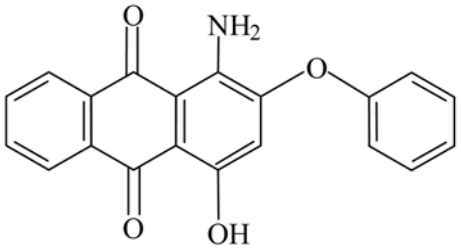

Fig. 1. Molecular structure of C. I. Disperse Red 60 dye.

EXPERIMENTAL

1. Materials

Pure DR60 dye (Fig. 1, molecular weight M=331 g/mol) that does not contain any dispersing agents was obtained from LG Chemicals (Korea) in a wet-cake form. The dye cakes were dried and ground into powder with diameters of 0.177-0.250 mm (60-80 mesh) before putting into the dyeing cell to improve its solubility in the supercritical fluids. Carbon dioxide of 99% in a cylinder equipped with a dip-tube was obtained from Daedong Oxygen (Korea). Extra pure grade of chlorobenzene was purchased from Janssen Chemicals (Germany). All these materials were used without further purification. Pellets of PS (molecular weight M=280,000 g/mol) and PMMA (molecular weight M=120,000 g/mol) (Fig. 2(a), (b); Aldrich Chemicals) were crafted into films by the solvent-casting method. The outgoing film thickness was 0.024 mm (1 mil). PET and Nylon 6 textiles (Fig. 2(c), (d)) were supplied from Shilla Textile (Korea) and Dongyang Nylon (Korea), respectively. Warp and weft of the textiles is 75 denier for both PET and Nylon 6 fibers and consists of 72 filaments for PET and 36 filaments for Nylon 6, respectively.

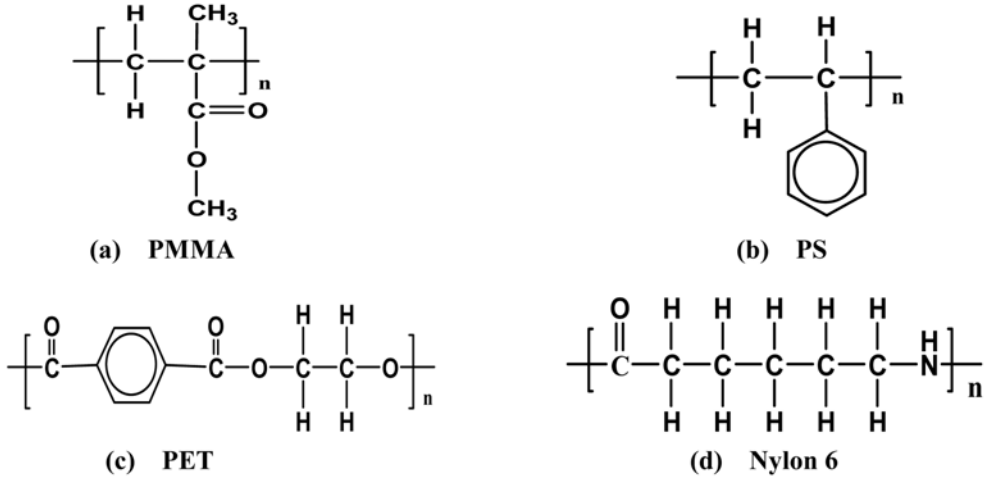

Fig. 2. Molecular structures of the polymers employed in this study.

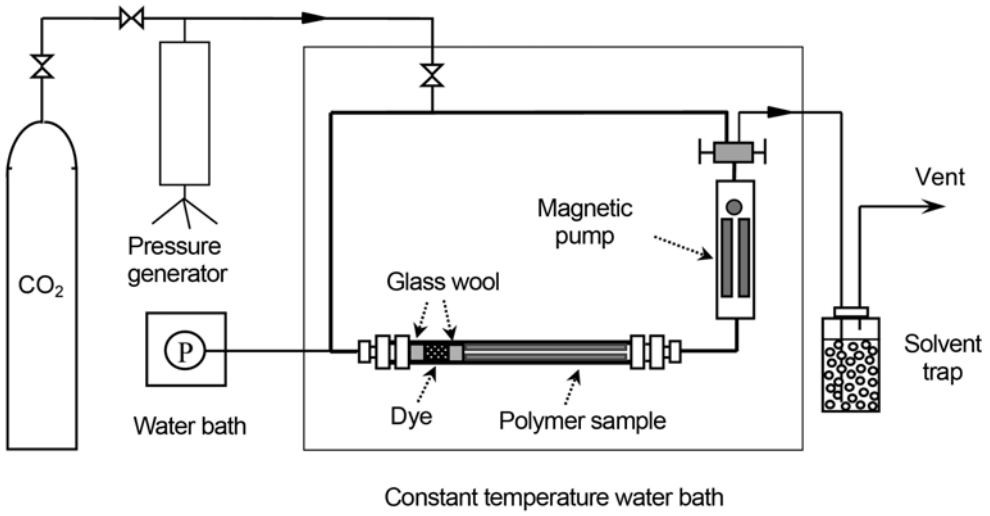

Fig. 3. Schematic diagram of the experimental closed-loop high-pressure sorption apparatus (P: pressure transducer).

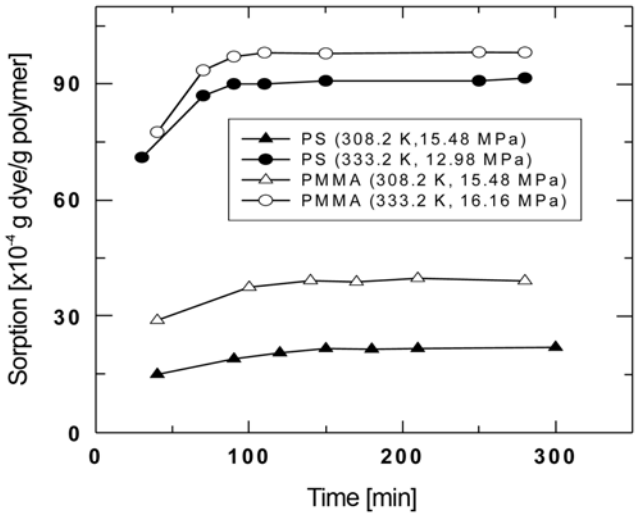

Fig. 4. Equilibrium sorption of DR60 in PS and PMMA films at 308.2 K and 333.2 K.

Table 1. Experimental and correlated sorption data for dual-mode sorption model for PS film

Temp. [K]	Pressure [MPa]	Density [g/ml]	Sorption [$\times 10^{-4}$ g dye/g polymer]	
			Experimental	Dual-mode
308.2	10.71	0.7367	14.00	14.68
	15.48	0.8217	21.67	19.77
	18.09	0.8498	22.96	22.35
	20.96	0.8743	25.78	25.05
	26.39	0.9105	29.73	29.87
	33.08	0.9446	33.04	35.41
313.2	10.33	0.6517	20.66	20.67
	17.21	0.8112	30.20	30.65
	24.13	0.8744	41.40	39.10
	30.95	0.9159	44.75	46.42
323.2	11.05	0.5097	52.08	55.12
	12.61	0.6192	61.05	59.30
	14.80	0.6952	66.48	64.52
	18.50	0.7651	76.71	72.05
	21.98	0.8072	78.54	78.06
	26.46	0.8467	84.47	84.75
	33.32	0.8911	88.08	93.46
333.2	6.65	0.1441	59.38	61.53
	8.46	0.2105	74.90	70.78
	11.60	0.4039	79.24	83.42
	12.98	0.5055	90.81	88.04
	16.16	0.6426	102.92	97.09
	22.54	0.7597	112.05	110.92
	30.12	0.8314	118.00	123.18
363.2	10.68	0.2230	161.22	168.19
	12.16	0.2703	181.08	177.00
	14.28	0.3454	193.06	187.67
	17.73	0.4675	207.64	201.52
	23.86	0.6171	220.38	219.61
	27.68	0.6755	224.53	228.28
	28.27	0.6830	230.59	229.49
	32.01	0.7248	230.06	236.60

The average diameter of each filament in PET fibers is 2.12 μ and that in Nylon 6 fibers is 3.29 μ.

2. Experimental Equipment and Procedures

A closed-loop high-pressure sorption apparatus (batch-type) circulated by a magnetic pump was placed in a constant-temperature air bath that could be controlled within ±1 K (Fig. 3) [14,40]. Prior to the experiment, a small amount of dye powder (about 1 g) was placed in one part (upstream side) of the cell, a tube made of stainless steel, with both ends plugged with glass wool, to prevent the dye powder from coming into the sorption cell. Then, polymer strips (0.4 cm×10 cm) or textile samples, separated by a thin wire screen to prevent the samples from contact directly with each other, were packed in the downstream side of the cell. After evacuating the entire loop, high-pressure carbon dioxide was introduced into the cell and then circulated in the loop with a magnetic pump. The magnetic pump consists of a small cylinder with a piston inside and a roll of concentric coil outside. As the piston continuously jumps up and down in the pump cylinder, the fluid is circulated along the loop at a rate of about 300 ml/min. A pressure gauge, consisting of a Senso-

Table 2. Experimental and correlated sorption data for dual-mode sorption model for PMMA film

Temp. [K]	Pressure [MPa]	Density [g/ml]	Sorption [$\times 10^{-4}$ g dye/g polymer]	
			Experiment	Dual-mode
308.2	10.71	0.7367	29.53	28.02
	15.48	0.8217	39.28	33.62
	18.09	0.8498	42.07	36.69
	20.96	0.8743	43.14	40.04
	26.39	0.9105	49.05	46.37
	33.08	0.9446	54.15	54.17
313.2	10.33	0.6517	38.14	38.25
	17.21	0.8112	50.83	50.93
	24.13	0.8744	63.31	61.55
	30.95	0.9159	69.63	71.06
323.3	11.05	0.5097	52.10	55.51
	12.61	0.6192	63.19	59.70
	18.50	0.7651	73.52	73.05
	22.84	0.8157	87.05	81.31
	23.07	0.8179	86.31	81.72
	26.46	0.8467	87.33	87.58
	32.39	0.8858	90.45	97.06
	33.32	0.8911	96.12	98.49
333.2	11.82	0.4211	81.72	83.49
	16.16	0.6426	98.12	96.30
	19.97	0.7236	109.75	105.46
	29.91	0.8299	121.76	124.79
	34.56	0.8612	131.37	132.54
363.2	10.68	0.2230	135.58	142.80
	12.16	0.2703	156.67	152.35
	14.28	0.3454	165.16	164.31
	14.98	0.3710	174.52	167.87
	17.73	0.4675	184.90	180.56
	23.86	0.6171	205.79	203.17
	26.04	0.6526	209.94	209.91
	33.12	0.7356	217.31	228.83

tec TJE pressure transducer and a GM signal conditioner/indicator, reads the pressure to ±0.014 MPa. At temperatures of 333.2 K and lower, it took about 250 min for PS and PMMA films (500 min for polyester and Nylon 6 textile samples) to get the sorption equilibrium. At temperatures of 363.2 K and above, however, it took much longer time to get the sorption equilibrium. Therefore, we kept PS and PMMA samples in the sorption cell for 500 to 900 min (8.3-15 h) and polyester and Nylon 6 textile samples for 1,200 to 2,000 min (20-33.3 h), depending upon temperature and pressure. When the sample cartridge had not been prepared properly, that is, leaving very small or even no space for the fluid to pass through, parts of the polymer were not dyed well, showing a color that was less bright than that of the other parts. In this case, we performed another experiment for a longer time with a newly prepared sample cartridge. After reaching the equilibrium sorption, the polymer strip samples were taken out of the cell and the dye micro-particles remaining on the surface of the strip were removed by using soap water. Then, the finished polymer sample was transferred into a beaker containing chlorobenzene at its boiling point (404.65 K) and kept there until the color of the polymer sample became clear and the dye was completely extracted from the polymer. After the polymer was taken out of the beaker, the dye concentration in the residual chlorobenzene solution was analyzed by a Perkin-Elmer Lambda 40 UV/Visible spectrometer. The light absorbance was measured at the primary spectral band of DR60 (wavelength of 515 nm). The solute concentration was determined from the calibration curve made using the Beer-Lambert law. The detailed experimental procedures are the same as reported previously [9]. The amount of sorption of dye in the polymer was calculated from the concentration of the dye in the chlorobenzene solution and the weights of both the polymer sample and chlorobenzene. The experimental error bound was estimated to about 6%.

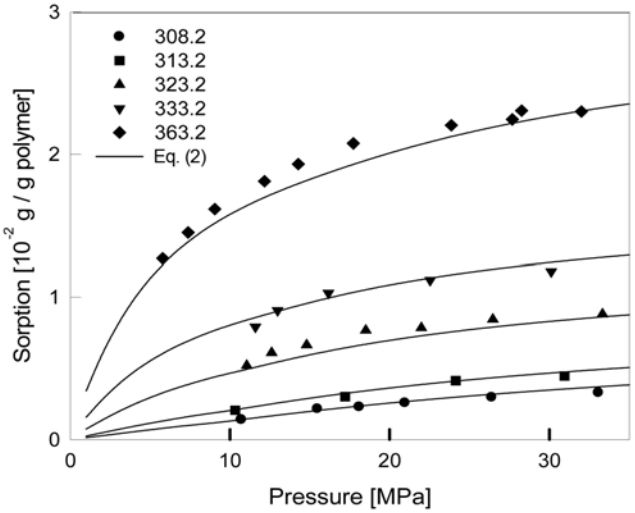

Fig. 5. Experimental sorption data correlated with Eq. (2) for the sorption of DR60 in PS film in the presence of supercritical CO_2.

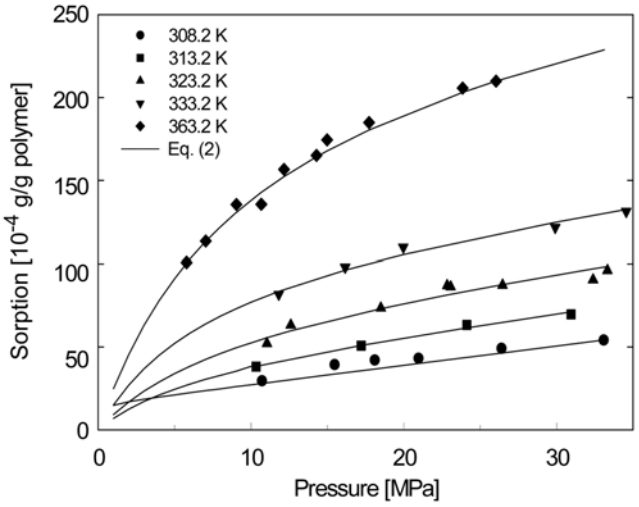

Fig. 6. Experimental sorption data correlated with Eq. (2) for the sorption of DR60 in PMMA film in the presence of supercritical CO_2.

RESULTS AND DISCUSSION

1. Sorption Equilibrium

The DR60 molecules are too large to penetrate into glassy polymers, such as PS and PMMA, because they behave like hard solids. When the polymer is exposed to a supercritical fluid, however, smaller

Table 3. Experimental and correlated sorption data for dual-mode sorption model for PET textile

Temp. [K]	Pressure [MPa]	Density [g/ml]	Sorption [$\times 10^{-4}$ g dye/g polymer]	
			Experiment	Dual-mode
333.2	11.13	0.3675	32.18	47.25
	12.11	0.4441	47.37	48.33
	14.78	0.5961	52.21	51.03
	17.92	0.6859	54.35	53.97
	25.54	0.7926	58.65	60.51
	28.60	0.8197	66.98	63.01
	33.74	0.8562	65.01	67.13
363.2	10.62	0.2213	88.77	95.96
	14.48	0.3525	128.58	114.01
	18.23	0.4832	133.05	128.01
	18.69	0.4974	137.65	129.58
	25.11	0.6382	142.28	148.00
	31.95	0.7243	149.93	163.37
393.2	10.51	0.1781	152.60	159.89
	14.64	0.2720	186.98	180.82
	14.70	0.2735	184.66	181.08
	18.32	0.3616	206.17	194.42
	24.82	0.5026	215.03	212.16
	32.46	0.6172	220.79	227.48
	33.97	0.6347	220.43	230.08
423.2	11.82	0.1768	272.39	282.60
	15.06	0.2352	315.58	308.94
	19.95	0.3266	361.91	312.31
	25.51	0.4244	377.25	345.46
	14.64	0.2276	316.42	372.85
	33.94	0.5432	382.01	402.79

fluid molecules easily penetrate into and widen the intermolecular spaces of the polymer, resulting in the characteristic swelling of the polymer. Thus, the swollen polymer becomes flexible [35], and the mobility of the polymer molecules is increased significantly, as shown with IR- and UV-spectroscopy by Kazarian et al. [36] and West et al. [28]. Therefore, large dye molecules dissolved in a supercritical fluid may easily diffuse into this swollen polymer. When the system is depressurized, the dye molecules are captured in the shrunken polymer structure, coloring it red. In supercritical fluid dyeing, the color intensity depends on the amount of dye uptake, which in turn is determined by pressure and temperature.

In Fig. 4, we do not see any appreciable increase in the dye sorption after 150 minutes. In each sorption measurement that is shown there, the amount of sorption after 300 minutes was only 3% larger than that after 150 minutes. Considering the leveling-off tendency of the sorption curve versus time, we assumed that the equilibrium sorption at an infinite time would be raised by less than 5%, compared with that at 150 minutes. Therefore, we did all sorption experiments for 200 minutes. In Tables 1 and 2 and Fig. 5 and 6, the amounts of sorption in the glassy polymers, i.e., PS and PMMA, increase with increasing pressure up to 35 MPa. This is because both the density of CO_2 and the solubility of dye in the fluid increase with increasing pressure. At high pressures, however, the rate of sorption was slowed down, indicating the polymer was about to be saturated with the dye molecules. At pressures below 5.0 MPa, we did not measure sorption, because the plasticization process was too slow and the equilibration took too much time. Up to 363.2 K, the amount of sorption increased nearly linearly with temperature at each pressure investigated.

Table 4. Experimental and correlated sorption data for dual-mode sorption model for Nylon 6 textile

Temp. [K]	Pressure [MPa]	Density [g/ml]	Sorption [$\times 10^{-4}$ g dye/g polymer]	
			Experiment	Dual-mode
363.2	11.13	0.2368	19.15	20.65
	14.48	0.3525	25.67	23.03
	18.23	0.4832	26.42	25.17
	25.11	0.6382	28.72	28.29
	25.67	0.6469	28.12	28.51
	31.95	0.7243	30.62	30.81
	32.57	0.7303	29.27	31.02
393.2	10.30	0.1736	31.35	34.24
	14.64	0.2720	43.83	40.56
	14.70	0.2735	44.00	40.63
	18.32	0.3616	47.65	44.61
	24.82	0.5026	49.95	50.09
	32.46	0.6172	52.23	54.94
	33.97	0.6347	52.20	55.76
423.2	11.82	0.1768	66.93	65.85
	15.06	0.2352	73.41	67.19
	19.95	0.3266	83.24	72.53
	25.41	0.4227	86.31	73.21
	11.21	0.1662	64.77	79.84
	14.64	0.2276	73.13	85.22
	33.94	0.5432	87.55	91.37

When the fluid penetrates into the bulk polymer, the polymer chains become more flexible. Therefore, as discussed in a previous paper [34], the glass transition temperature, T_g, of a polymer is greatly reduced when the pressure of the system goes up much higher. Wissinger and Paulaitis [37] showed that T_g of PMMA was reduced from 378 K to 333 K when one gram of PMMA absorbed 40 ml (measured at 273.2 K and 101.3 kPa) of CO_2. They reported that 110 ml (STP) of CO_2 was absorbed in one gram of PMMA at 10 MPa and 332 K [37]. Chang et al. [34] reported that 218 ml (STP) of CO_2 was absorbed in one gram of PMMA at 20 MPa and 323 K. For PS at 20 MPa and 323 K, 71 ml (STP) of CO_2 was absorbed in one gram of polymer, shifting T_g down by 90 K from 373 to 283 K [37]. Thus, we may say that both PMMA and PS were transformed from their glassy states to the rubbery states within the entire experimen-

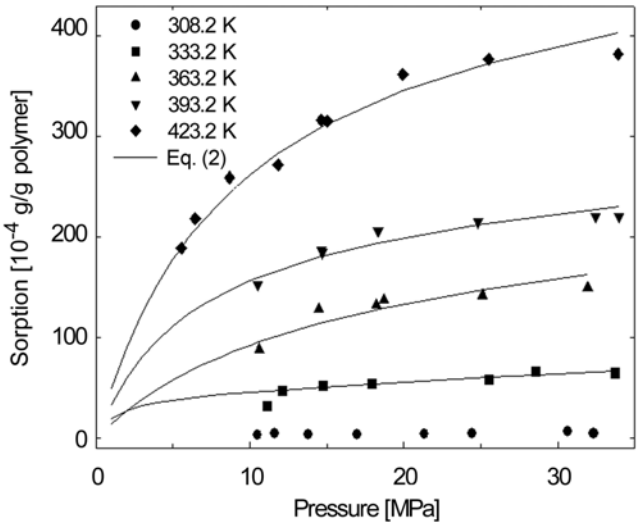

Fig. 7. Experimental sorption data correlated with Eq. (2) for the sorption of DR60 in PET textile in the presence of supercritical CO_2.

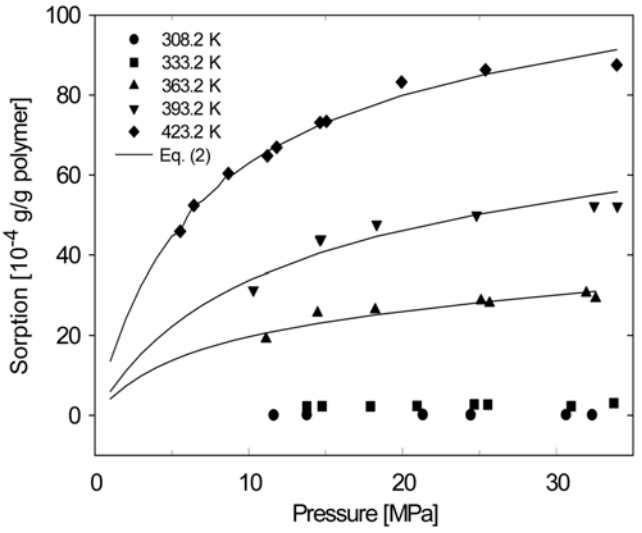

Fig. 8. Experimental sorption data correlated with Eq. (2) for the sorption of DR60 in Nylon 6 textile in the presence of supercritical CO_2.

tal conditions of this study. Above T_g, the amount of dye sorption increased linearly with temperature, mainly due to the increase of dye solubility caused by the increasing temperature of the supercritical fluid.

For PS and PMMA, the amount of dye sorption at 30 MPa and 363.2 K is almost the same: 0.023 and 0.022 g/g polymer, respectively. Due to the benzyl groups in the polymer chain, PS has a larger intermolecular space as well a better intermolecular (aromatic) interaction with DR60 than PMMA which does not have any aromatic group (see Fig. 2(a) and (b)). Note that DR60 has an (aromatic) an-

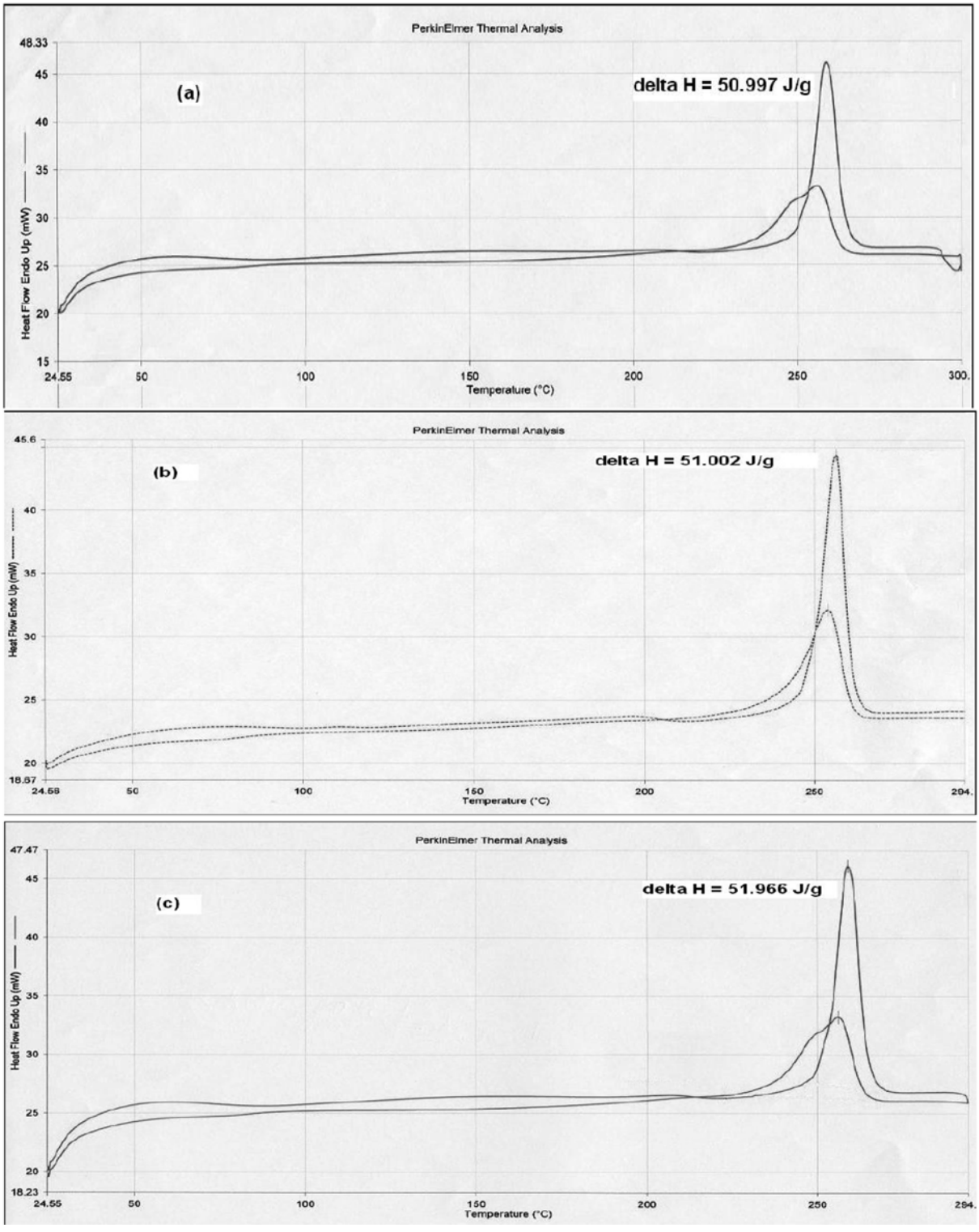

Fig. 9. DSC curves for PET samples: (a) untreated, (b) dyed with DR60 in supercritical CO_2, and (c) treated in supercritical CO_2 without DR60.

thraquinone group as well. Therefore, the DR60 molecules can get into the polymer structure more easily. However, DR60 has two strong polar groups (-NH_2 and -OH) that can form hydrogen bonds with oxygen atoms in the carboxylate groups of the PMMA molecules, lending better chemical affinity to PMMA than to PS. The formation of hydrogen-bonding between PMMA and C. I. Disperse Red 1 (DR1) dye (an azo-derivative) was verified by Kazarian et al. [36] using IR-spectroscopy. The combined structural and chemical effect on the sorption of polar dye results in almost the same degree of sorption of DR60 for the glassy polymers PMMA and PS.

Tables 3 and 4 and Fig. 7 and 8 show that the amount of sorption of DR60 dye in crystalline PET and Nylon 6 textile fibers at 30 MPa and 363.2 K amounts to about 0.015 and 0.0032 g/g polymer, respectively. These values are 35% and 86% smaller than the sorption in PS even though the general sorption behavior looks almost the same. The polymeric crystal lattice is so closely packed that neither bulky dye molecules nor smaller CO_2 molecules can penetrate into. However, the amorphous part between the crystalline structures of the polymer could behave in the same manner as other pure glassy polymers. It is well known that the smaller sorption values in these crystalline polymers are due to their high crystallinity. Note that PET and Nylon 6 have high degrees of crystallinity of 30% and 60%, respectively. As can be expected from Fig. 2(c) and (d), Nylon 6, which consists of a straight chain without any bulky aromatic groups, has a twofold higher crystallinity than PET and thus displays only $1/5^{th}$ of the dye sorption of PET. At 30 MPa and 423.2 K, the amount of sorption of PET textile was considerably larger than that was expected based on the data at 393.2 K, indicating that the polymer became much more flexible. The glass transition temperature of crystalline PET of 354.2 K (398.2 K for the crystalline and oriented PET [38]) must have been shifted down by at least 20 to 30 K, as the absorbed CO_2 molecules plasticized the polymer. Plasticization enhances the dye uptake capability of polyester fibers. Using wide-angle X-ray scattering measurements, Sfiligoj and Zipper [39] showed that supercritical CO_2 augments the total crystallinity by the formation of new crystalline regions and that the existing crystallites diminish, yielding smaller or less perfect crystallites. Therefore, degrees of crystallinity of PET and Nylon 6 could be changed during the sorption process. Furthermore, the melting point of the polymer can be correlated with the crystallinity. Differential scanning calorimetry (DSC) was applied for some PET samples at different conditions (Fig. 9). Here, the higher peaks for each sample were obtained from the first scan and the lower peaks, from the second scan, respectively. As the commercial textile fibers are normally crystallized at over 473 K, each fiber must have a sharp peak. Since the values for the enthalpy change of fusion for all the samples are almost the same (within the experimental uncertainty), we can say the fibers are not influenced by the supercritical fluid treatment at 30.0 MPa and 373 K for 60 min or by dyeing at the same supercritical fluid condition. Among the peaks from the second scan the one for the dyed PET textile fiber (Fig. 9(d)) appears different from others. Because a disperse dye can act as a nucleus of the crystalline structure making more crystals, the second peak becomes narrower than those obtained from the treatment with CO_2 only. However, to fully understand the effect of high-pressure CO_2 in the crystallinity of polymers, we need further research in this area.

2. Analysis with a Quasi Dual-mode Sorption Model

All the sorption isotherms for large dye molecules in Fig. 5-8 show a behavior that conforms with the dual-mode model proposed by Fleming and Koros [35] for the sorption of small CO_2 molecules. Chang et al. [34] found the same sorption behavior for CO_2 in polycarbonate at pressures up to 10 MPa. Some solute molecules are adsorbed onto the surface of micro-voids of the polymer (Langmuir adsorption), while some others are absorbed into the polymer matrix (Henry absorption). The adsorption is believed to occur only at low pressures. The surfaces of micro-voids are then completely covered with dye molecules at about 3.0 MPa, leaving no surface for further adsorption at higher pressures. Chang et al. [34] showed similar behavior for CO_2 sorption. Therefore, we can conclude that the major sorption mechanism is absorption in the free volume of the polymer matrix. The leveling-off behavior in Fig. 5-8 must have occurred as the free volume was gradually consumed by the dye molecules. Smaller CO_2 molecules can easily penetrate into the free volume of the polymer matrix and swell the polymer, promoting the diffusion of the dye molecules in the polymer [3]. There may be some competition between the absorbed CO_2 molecules and the penetrating dye molecules during the sorption process. The bulky dye molecules pertaining to stronger intermolecular interaction with

Table 5. Values of the model parameters obtained by correlating the data for PS film

Temp. [K]	Pressure [MPa]	k_L	C_m	k_{23}
308.2	10.71	11.265	0.00258	8501
	15.48	10.483	0.00258	7911
	18.09	9.875	0.00258	7452
	20.96	9.181	0.00258	6928
	26.39	7.893	0.00258	5956
	33.08	6.461	0.00258	4875
313.2	10.33	6.291	0.00506	4220
	17.21	5.623	0.00506	3772
	24.13	4.657	0.00506	3124
	30.95	3.792	0.00506	2544
323.2	11.05	2.065	0.00978	3156
	12.61	2.056	0.00978	3143
	14.80	1.978	0.00978	3024
	18.50	1.800	0.00978	2752
	21.98	1.627	0.00978	2487
	26.46	1.417	0.00978	2166
	33.32	1.137	0.00978	1738
333.2	11.60	0.7259	0.0136	1352
	12.98	0.7263	0.0136	1353
	16.16	0.6864	0.0136	1278
	22.54	0.5688	0.0136	1059
	30.12	0.4434	0.0136	826
363.2	10.68	0.0435	0.0284	108.7
	12.16	0.0446	0.0284	110.4
	14.28	0.0450	0.0284	111.3
	17.73	0.0430	0.0284	106.6
	23.86	0.0361	0.0284	89.4
	27.68	0.0316	0.0284	78.3
	28.27	0.0310	0.0284	76.7
	32.01	0.0271	0.0284	67.1

polymer molecules can easily replace the smaller and weaker interacting CO_2 molecules. The large dye molecules squeeze into the polymer matrix, making more spaces for smaller CO_2 molecules. The replaced CO_2 molecules may stay nearby within the polymer. Since there has not yet been a proper model to analyze that particular sorption behavior, we tried to use a sorption equation similar to the dual-mode model, shown below, within our experimental conditions:

$$C = k_L P + \frac{C_m k_N P}{(1 + k_N P)} \quad (1)$$

where C is the amount of sorption, P is the pressure, k_L is the constant for the linear contribution to the sorption, k_N is the constant for the nonlinear contribution, and C_m is the maximum amount of sorption.

Since Eq. (1) is not suitable for high-pressure applications but for the sorption of pure low-pressure gas, an alternative equation in the form of Langmuir equation was derived from the high-pressure equilibrium-adsorption correlation using the fugacity coefficients for CO_2 and the solute for a more accurate analysis. This quasi-Langmuir adsorption indicates the adsorption on the surface of the polymer's micro-voids. Then, Henry absorption in the polymer matrix

Table 6. Values of the model parameters obtained by correlating the data for PMMA film

Temp. [K]	Pressure [MPa]	k_L	C_m	k_{23}
308.2	10.71	23.14	0.00158	1260000
	15.48	21.54	0.00158	1173000
	18.09	20.29	0.00158	1105000
	20.96	18.86	0.00158	1027000
	26.39	16.21	0.00158	883200
	33.08	13.27	0.00158	722900
313.2	10.33	12.82	0.00422	17540
	17.21	11.46	0.00422	15670
	24.13	9.49	0.00422	12980
	30.95	7.73	0.00422	10570
323.2	11.05	4.146	0.00746	4312
	12.61	4.127	0.00746	4293
	18.50	3.614	0.00746	3759
	22.84	3.183	0.00746	3310
	23.07	3.160	0.00746	3287
	26.46	2.844	0.00746	2958
	32.39	2.353	0.00746	2447
	33.32	2.282	0.00746	2374
333.2	11.82	1.439	0.0111	1768
	16.16	1.359	0.0111	1669
	19.97	1.220	0.0111	1499
	29.91	0.884	0.0111	1086
	34.56	0.756	0.0111	929
363.2	10.68	0.0829	0.0244	76.9
	12.16	0.0850	0.0244	78.8
	14.28	0.0857	0.0244	79.5
	14.98	0.0854	0.0244	79.2
	17.73	0.0820	0.0244	76.1
	23.86	0.0688	0.0244	63.8
	26.04	0.0638	0.0244	59.2
	33.12	0.0496	0.0244	46.0

Table 7. Values of the model parameters obtained by correlating the data for PET textile

Temp. [K]	Pressure [MPa]	k_L	C_m	k_{23}
333.2	11.13	0.9167	0.00436	9171
	12.11	0.9237	0.00436	9240
	14.78	0.8987	0.00436	8990
	17.92	0.8310	0.00436	8313
	25.54	0.6549	0.00436	6551
	28.60	0.5919	0.00436	5921
	33.74	0.4981	0.00436	4983
363.2	10.62	0.0531	0.0197	54.16
	14.48	0.0549	0.0197	56.03
	18.23	0.0520	0.0197	53.10
	18.69	0.0515	0.0197	52.52
	25.11	0.0423	0.0197	43.15
	31.95	0.0332	0.0197	33.87
393.2	10.51	0.00477	0.0242	10.24
	14.64	0.00506	0.0242	10.87
	14.70	0.00506	0.0242	10.87
	18.32	0.00494	0.0242	10.60
	24.82	0.00424	0.0242	9.11
	32.46	0.00329	0.0242	7.06
	33.97	0.00312	0.0242	6.69
423.2	11.82	0.000628	0.0473	0.979
	15.06	0.000654	0.0473	1.020
	19.95	0.000656	0.0473	1.023
	25.51	0.000640	0.0473	0.998
	14.64	0.000573	0.0473	0.893
	33.94	0.000445	0.0473	0.694

Table 8. Values of the model parameters obtained by correlating the data for Nylon 6 textile

Temp. [K]	Pressure [MPa]	k_L	C_m	k_{23}
363.2	11.13	0.01640	0.00283	116.20
	14.48	0.01560	0.00283	118.90
	18.23	0.01270	0.00283	112.70
	25.11	0.01240	0.00283	91.56
	25.67	0.00994	0.00283	89.83
	31.95	0.00972	0.00283	71.87
	32.57	0.00966	0.00283	70.31
393.2	10.30	0.00142	0.00619	6.585
	14.64	0.00152	0.00619	7.036
	14.70	0.00152	0.00619	7.037
	18.32	0.00148	0.00619	6.864
	24.82	0.00127	0.00619	5.899
	32.46	0.00099	0.00619	4.572
	33.97	0.00093	0.00619	4.333
423.2	11.82	0.000185	0.0100	1.291
	15.06	0.000188	0.0100	1.311
	19.95	0.000196	0.0100	1.366
	25.41	0.000196	0.0100	1.370
	11.21	0.000192	0.0100	1.336
	14.64	0.000172	0.0100	1.199
	33.94	0.000133	0.0100	0.929

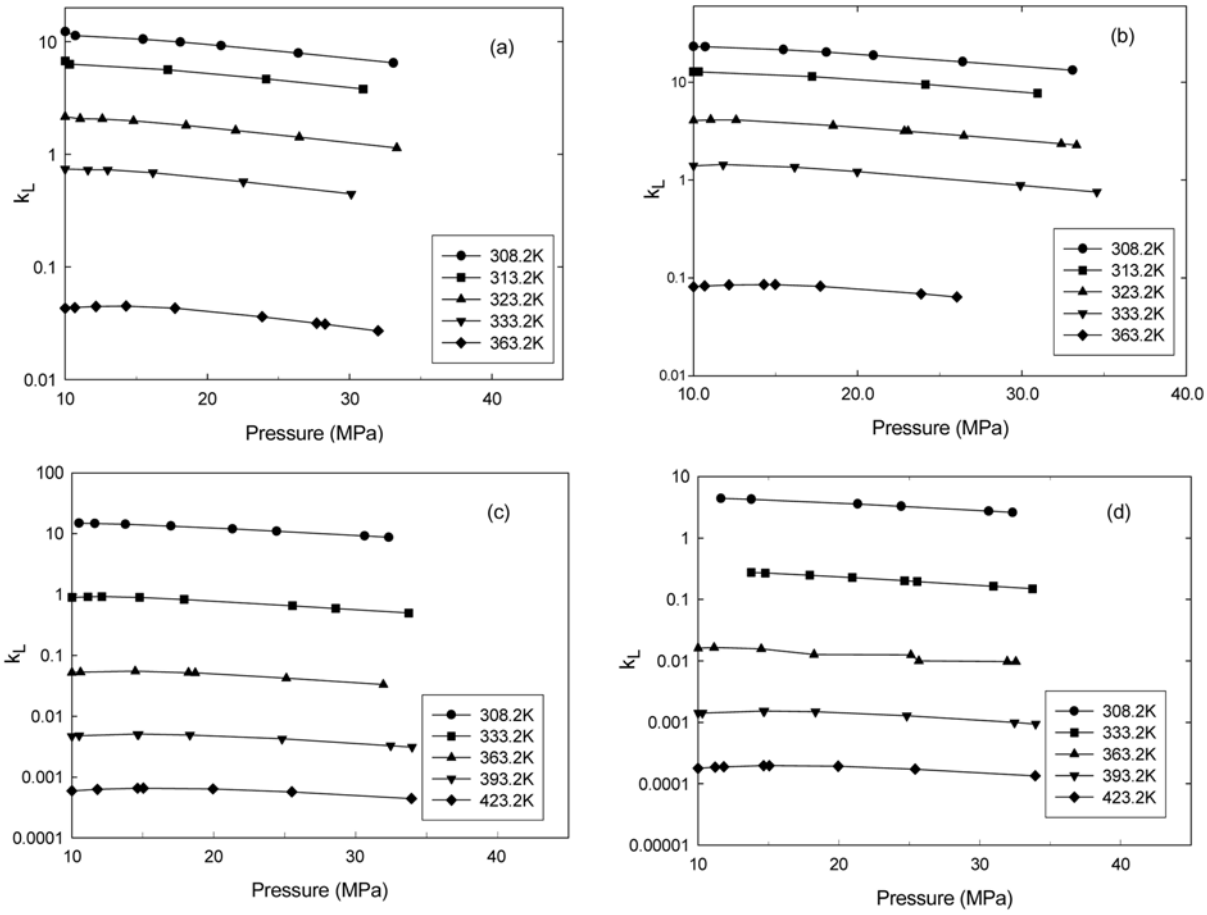

Fig. 10. Linear sorption constant k_L in Eq. (2) as a function of pressure for (a) PS film, (b) PMMA film, (c) PET textile, and (d) Nylon 6.

was added to this quasi-Langmuir adsorption to cover the entire sorption that takes place in the polymer:

$$C = k_L y_2 \phi_2 P + \frac{C_m k_{23} y_2 \phi_2 P}{1 + k_{23} y_2 \phi_2 P + k_{13} y_1 \phi_1 P} \quad (2)$$

where y_2 is the mole fraction of the solute, ϕ_1 is the fugacity coefficient of the fluid, ϕ_2 is the fugacity coefficient of the solute, k_{13} is the Langmuir constant related to the fluid-polymer interaction, and k_{23} is the Langmuir constant related to the solute-polymer interaction. Subscripts 1, 2, and 3 designate CO_2, dye, and polymer, respectively. Note that, in the denominator of the second term of the right side of Eq. (2), we have an additional term, $k_{13}y_1\phi_1P$, to reflect the sorption of CO_2. Dye solubility y_2 was obtained from the literature [40], and the fugacity coefficients were calculated using the Peng-Robinson equation of state. The energy parameter a in the Peng-Robinson equation of state is normally evaluated from the critical properties of the fluid and the solute. Due to its high molecular weight, DR60 must have a very high critical pressure as well as a very high critical temperature, and it may be impossible for DR60 to reach its critical temperature before being decomposed. Therefore, the critical properties of DR60 are not available in the literature and impossible to obtain experimentally. Its vapor pressure is also too small to measure. Therefore, the only way to obtain the Peng-Robinson energy parameter is to correlate the experimental sorption data for DR60 with the equation. The first term, $k_1y_2\phi_2P$, on the right side of Eq. (2) is to describe the linearly increasing sorption behavior, and the second term is to describe the corresponding nonlinear behavior. The linear sorption constant k_L (shown in Tables 5-8), which was evaluated from the dye-sorption data at high pressures, shows slightly decreasing behavior with pressure for all temperatures (Fig. 10). The contribution of the group $k_{13}y_1\phi_1P$ in the denominator of the second term is relatively small and thus may be neglected in the calculation. At high pressures, the free volume of polymer is filled up with CO_2 molecules and the solute molecules. Since filling the micro-voids or free-volume in the polymer matrix may be different from adsorption on the pore-surface, we put the prefix "quasi" to indicate that we do not have a solid theoretical background yet.

The other constants were evaluated by rearranging the second term in Eq. (2) (let us denote it as C′) to consider the nonlinear contribution to the sorption as follows:

$$\frac{1}{C'} = \frac{1}{C_m k_{23} y_2 \phi_2} \cdot \frac{1}{P} + \frac{1}{C_m} \quad (3)$$

The constants C_m and k_{23} (Tables 5-8) were calculated from the slope and the intercept obtained from a plot of 1/C′ vs. 1/P (Fig. 11). The maximum amount of sorption C_m increases linearly with temperature for both PMMA and PS (Fig. 12). This is mainly due to the increase in the solubility of dye with increasing temperature. The constant for solute-polymer interaction, k_{23}, shows a slightly decreasing tendency with pressure as shown in Fig. 13. Parameters for the

other polymers were obtained in a similar way. The sorption values calculated by the quasi-dual mode sorption model using these parameters (Tables 1-4) are drawn as solid lines in Fig. 5-8. Once we know the parameters of this model, we can predict the amount of sorption at any conditions. The correlated model equation now minimizes the number of necessary experiments that are required in developing a new supercritical fluid dyeing process, lowering the initial

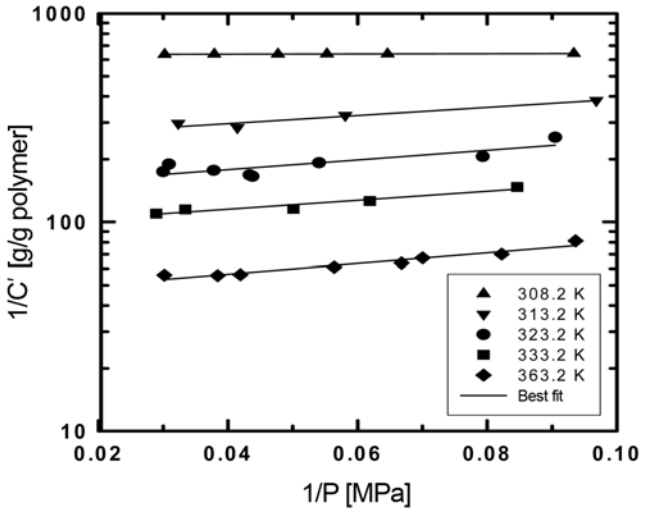

Fig. 11. A plot to evaluate C_m and k_{23} values in Eq. (3) for the sorption of DR60 in the PMMA film in the presence of supercritical CO_2.

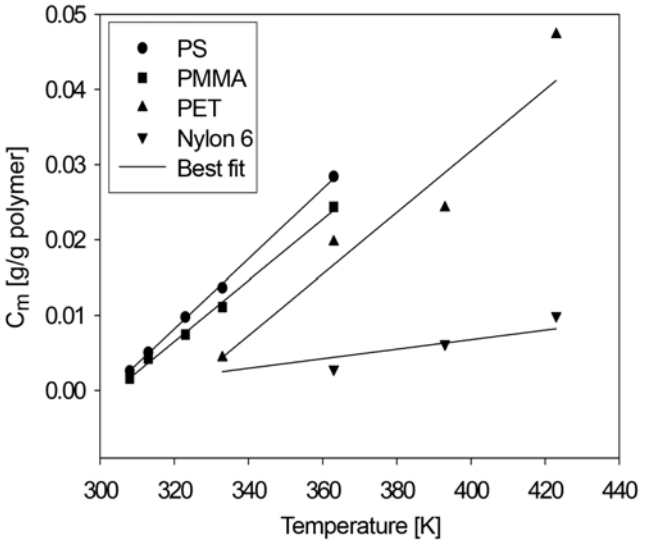

Fig. 12. Values of constant C_m in Eq. (3) as a function of temperature for PS and PMMA films and PET and Nylon 6 textile, respectively.

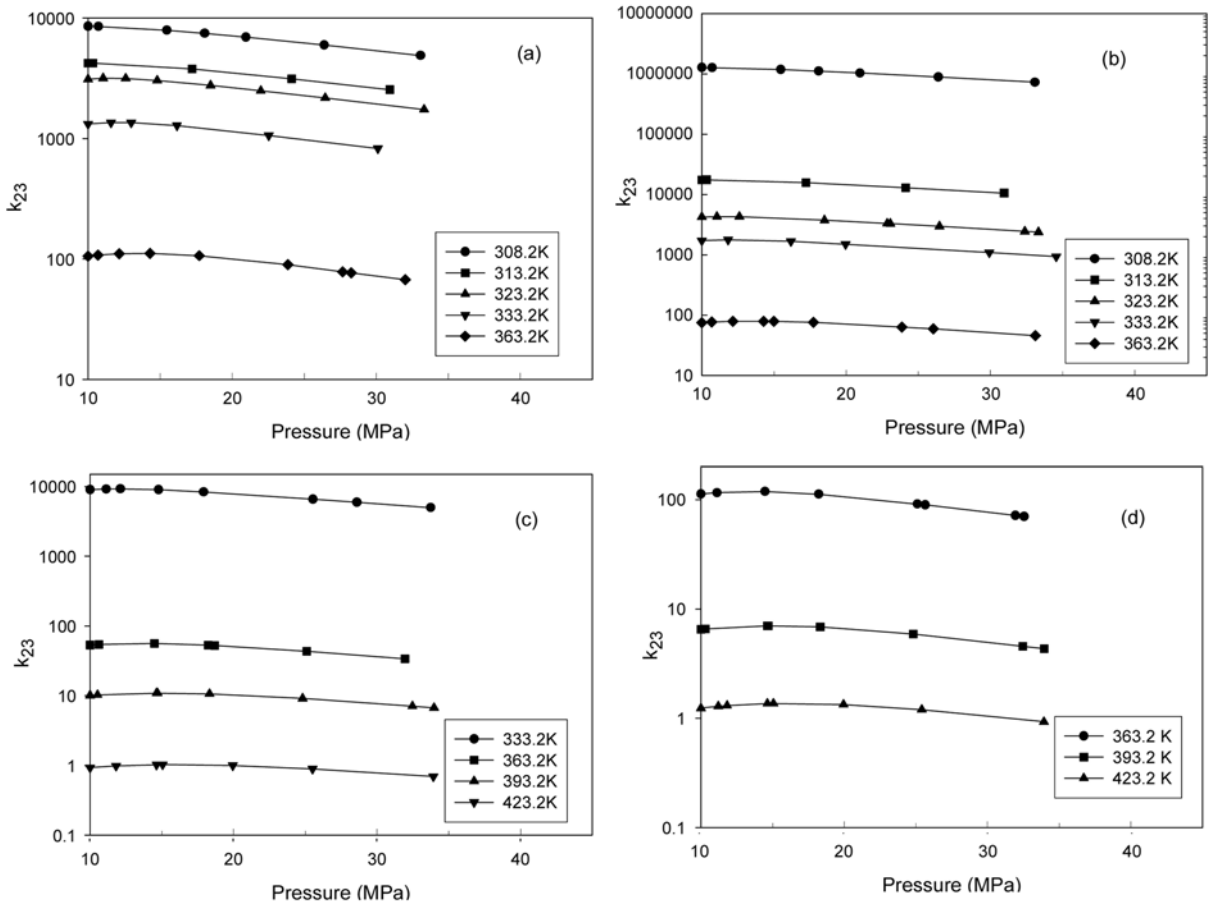

Fig. 13. Solute-polymer interaction constant k_{23} in Eq. (2) as a function of pressure for (a) PS, (b) PMMA films and (c) PET, (d) Nylon 6 textile.

investment cost.

CONCLUSIONS

The amount of sorption of DR60 in supercritical CO_2 monotonically increased with pressure at a constant temperature and increased with temperature at a constant pressure for glassy polymer films, PS and PMMA, and crystalline polymer textiles, PET and Nylon 6, respectively. The rate of sorption decreased with increasing pressure. The strong interactions due to the hydrogen-bond formation between dye and polymer molecules as well as the amount of interpolymer chain spaces may have significantly influenced the sorption of dye in the polymer. The relatively large amount of sorption at temperatures lower than T_g and high pressure might have been due to the T_g depression of the CO_2-swollen polymers. The lower sorption in the crystalline PET and Nylon 6 fibers than in the glassy PS and PMMA films was due to their higher degrees of crystallinity. An equation similar to the dual-mode sorption model that was derived from a high-pressure equilibrium correlation is able to predict the sorption successfully at any other conditions.

ACKNOWLEDGMENT

This research was supported by Yeungnam University Research Grant 2007.

REFERENCES

1. M. A. McHugh and V. J. Krukonis, *Supercritical fluid extraction: Principles and practice*, 2nd ed., Butterworth-Heinemann, Boston (1994).
2. J. L. Kendall, D. A. Canelas, J. L. Young and J. M. DeSimone, *Chem. Rev.*, **99**(2), 543 (1999).
3. J.-Y. Park and J.-J. Shim, *J. Supercrit. Fluids*, **27**(3), 297 (2003).
4. J.-J. Shim and K. P. Johnston, *AIChE J.*, **35**(7), 1097 (1989).
5. A. R. Berens, G. S. Huvard and R. W. Korsmeyer, Paper No. 48b, AIChE Meeting, Washington, D.C. (1988).
6. W. Saus, D. Knittel and E. Schollmeyer, *Textile Res. J.*, **63**(3), 135 (1993).
7. D. Knittel, W. Saus and E. Schollmeyer, *J. Text. Inst.*, **84**(4), 534 (1993).
8. B. Gebert, W. Saus, D. Knittel, H.-J. Buschmann and E. Schollmeyer, *Textile Res. J.*, **64**(7), 371 (1994).
9. K.-H. Chang, H.-K. Bae and J.-J. Shim, *Korean J. Chem. Eng.*, **13**(3), 310 (1996).
10. E. Bach, E. Cleve and E. Schollmeyer, *J. Text. Inst.*, **89**(4), 657 (1998).
11. E. Bach, E. Cleve and E. Schollmeyer, *J. Text. Inst.*, **89**(4), 647 (1998).
12. B. Shannon, W. Hendrix, B. Smith and G. Montero, *J. Supercrit. Fluids*, **19**(1), 87 (2000).
13. G. A. Montero, C. B. Smith, W. A. Hendrix and D. L. Butcher, *Ind. Eng. Chem. Res.*, **39**(12), 4806 (2000).
14. P. Muthukumaran, R. B. Gupta, H.-D. Sung, J.-J. Shim and H.-K. Bae, *Korean J. Chem. Eng.*, **16**(1), 111 (1999).
15. A. S. Özcan, A. A. Clifford, K. D. Bartle and D. M. Lewis, *J. Chem. Eng. Data*, **42**(3)**,** 590 (1997).
16. J.-J. Shim and H.-D. Sung, Proceedings of the 4th International Symposium on Supercritical Fluids, Sendai, Japan, 467 (1997).
17. P. Swidersky, D. Tuma and G. M. Schneider, *J. Supercrit. Fluids*, **9**(1-3), 12 (1996).
18. D. Tuma and G. M. Schneider, *J. Supercrit. Fluids*, **13**(1-3), 37 (1998).
19. D. Tuma and G. M. Schneider, *Fluid Phase Equilibr.*, **158-160,** 743 (1998).
20. D. Tuma, B. Wagner and G. M. Schneider, *Fluid Phase Equilibr.*, **182**(1-2), 133 (2001).
21. E. Bach, E. Cleve, J. Schüttken, E. Schollmeyer and J. W. Rücker, *Color. Technol.*, **117**(1), 13 (2001).
22. B. Wagner, C. B. Kautz and G. M. Schneider, *Fluid Phase Equilibr.*, **158-160**, 707 (1999).
23. J.-K. Baek, M. S. Thesis, Yeungnam University, Korea (2001).
24. J.-K. Baek, S. Kim, G-S. Lee and J.-J. Shim, *Korean J. Chem. Eng.*, **21**(1), 230 (2004).
25. Z. Huang, Y.-H. Guo, G.-B. Sun, Y. C. Chiew and S. Kawi, *Fluid Phase Equilibr.*, **236**(1-2), 136 (2005).
26. M. D. Gordillo, C. Pereyra and E. J. Martínez de la Ossa, *Dyes Pigments*, **67**(3), 167 (2005).
27. U. Haarhaus, P. Swidersky and G. M. Schneider, *J. Supercrit. Fluids*, **8**(2), 100 (1995).
28. B. L. West, S. G. Kazarian, M. F. Vincent, N. H. Brantley and C. A. Eckert, *J. Appl. Polym. Sci.*, **69**(5), 911 (1998).
29. O. S. Fleming, F. Stepanek and S. G. Kazarian, *Macromol. Chem. Phys.*, **206**(11), 1077 (2005).
30. W. L. F. Santos, A. P. Moura, N. P. Povh, E. C. Muniz and A. F. Rubira, *Macromol. Symp.*, **229**(1), 150 (2005).
31. A. J. Seckner, A. K. McClellan and M. A. McHugh, *AIChE J.*, **34**(1), 9 (1988).
32. J.-J. Shim and K. P. Johnston, *AIChE J.*, **37(**4), 607 (1991).
33. J.-J. Shim and K. P. Johnston, *J. Phys. Chem.*, **95**(1), 353 (1991).
34. S.-H. Chang, S.-C. Park and J.-J. Shim, *J. Supercrit. Fluids*, **13** (1-3), 113 (1998).
35. G. K. Fleming and W. J. Koros, *Macromolecules*, **19**(8), 2285 (1986).
36. S. G. Kazarian, N. H. Brantley, B. L. West, M. F. Vincent and C. A. Eckert, *Applied Spectrosc.*, **51**(4), 491 (1997).
37. R. G. Wissinger and M. E. Paulaitis, *J. Polym. Sci. Part B: Polym. Phys.*, **25**(12), 2497 (1987).
38. J. Brandrup, E. H. Immergut and E. A. Grulke, *Polymer handbook*, 4th ed., John Wiley & Sons, New York (1999).
39. M. S. Sfiligoj and P. Zipper, *Colloid Polym. Sci.*, **276**(2), 144 (1998).
40. H.-D. Sung and J.-J. Shim, *J. Chem. Eng. Data*, **44**(5), 985 (1999).